Quenching Spin Diffusion in Selective Measurements of Transient Overhauser Effects in Nuclear Magnetic Resonance. Applications to Oligonucleotides†

Catherine Zwahlen,‡ Sébastien J. F. Vincent,‡ Lorenzo Di Bari,§ Malcolm H. Levitt,⊥ and Geoffrey Bodenhausen*,‡

Contribution from the Section de Chimie, Université de Lausanne, Rue de la Barre 2, CH-1005 Lausanne, Switzerland, Dipartimento di chimica e chimica industriale, Università degli studi di Pisa, Via Risorgimento 35, I-56126 Pisa, Italy, and Division of Physical Chemistry, Arrhenius Laboratory, University of Stockholm, S-10691 Stockholm, Sweden

Received August 14, 1993®

Abstract: In high-resolution nuclear magnetic resonance (NMR), the transfer of longitudinal magnetization from one spin to another (A ⇝ X) under the effect of cross relaxation (nuclear Overhauser effect) is often complicated by spin-diffusion pathways through other spins K in the vicinity (e.g., A ⇝ K ⇝ X). It is shown how these undesirable pathways can be quenched by manipulating the magnetization of the two sites A and X with doubly selective inversion pulses. At the beginning of the experiment, after selective inversion of the "source" spin A, the longitudinal magnetization tends to migrate not only to the "target" nucleus X but also to various other "clandestine" nuclei K, K′, ... ($\langle I_z^A \rangle$ ⇝ $\langle I_z^K \rangle$, $\langle I_z^{K'} \rangle$, ...). In the middle of the interval τ_m, the longitudinal magnetization components of both A and X are inverted simultaneously, without affecting the spins K, K′, ... The direct flow of magnetization from A to X is not perturbed by this manipulation, but the indirect flow via K, K′, ... is reversed in sign and almost perfectly canceled at the end of the relaxation interval τ_m. If the signal of the target spin X overlaps with other resonances, the polarization $\langle I_z^X \rangle$ may be monitored indirectly by a doubly selective magnetization transfer to a "spy" proton M through a scalar coupling J_{MX}. The methods are illustrated by applications to Overhauser effects in the palindromic deoxyribonucleic acid d(CGCGAATTCGCG)$_2$, which forms a B-type double helix.

Introduction

Although two-dimensional nuclear Overhauser spectroscopy (NOESY)[1-6] provides a remarkably effective tool for investigating cross relaxation in macromolecules, it is known that the spectra can be misleading if spin-diffusion effects are not properly taken into account.[6-12] Only to first order in the relaxation time τ_m is the amplitude a_{AX} of a NOESY cross peak directly proportional to the cross-relaxation rate σ_{AX} and therefore related to the internuclear distance r_{AX}. To second order in τ_m, however, the amplitude of a cross peak is also affected by products of cross-relaxation rates $\sigma_{AK}\sigma_{KX}$, $\sigma_{AK'}\sigma_{K'X}$, etc. These signal contributions arise from two-step "spin-diffusion" processes A ⇝ K ⇝ X, A ⇝ K′ ⇝ X, etc. If the duration of the τ_m interval is increased, one also observes n-step processes with contributions proportional to τ_m^n. To gain insight into the extent of spin diffusion, one may record so-called "buildup" curves to monitor the cross peak amplitudes a_{AX} as a function of the mixing time τ_m.[8] Such curves can be obtained either from a series of two-dimensional NOESY spectra or from one-dimensional QUICK-NOESY experiments.[13] These buildup plots can be simulated and fitted quantitatively by considering the simultaneous effect of all cross-relaxation rates σ_{ij}, using the "full relaxation matrix" method.[14,15] However, even if one can predict the amplitudes a_{AX} once all rates σ_{AX}, σ_{AK}, σ_{KX}, etc. are known, this does not necessarily imply that it is possible to obtain accurate estimates of all cross-relaxation rates σ_{AX} from the amplitudes a_{AX} in the presence of noise and instrumental imperfections. This drawback applies particularly to small cross-relaxation rates, which are often of particular significance for structural determination since they tend to refer to longer distances. Clearly, the accuracy of the determination of σ_{AX} would be greatly improved if spin diffusion could be quenched[10-12] so that the cross peak amplitude $a_{AX}(\tau_m)$ would depend *only* on the rate σ_{AX}.

Several groups have attacked this problem in different ways, but none of the proposals made so far seems to be truly satisfactory. Olejniczak et al.,[10] Massefski and Redfield,[11] and Fejzo et al.[12] have demonstrated that, provided the dispersion of the chemical shifts is favorable, spin-diffusion via "clandestine" spins in a selected spectral region may be inhibited by irradiation with a continuous radio frequency (rf) or with a sequence of π pulses. Macura and co-workers,[16,17] on the other hand, used a combination of spin-locking fields and selective π pulses to suppress, at least

† Dedicated to Professor Richard R. Ernst, Zürich, on the occasion of his 60th birthday.

‡ Université de Lausanne.

§ Università degli studi di Pisa.

⊥ University of Stockholm.

® Abstract published in *Advance ACS Abstracts,* December 15, 1993.

(1) Meier, B. H.; Ernst, R. R. *J. Am. Chem. Soc.* **1979**, *101*, 6441.
(2) Jeener, J.; Meier, B. H.; Bachmann, P.; Ernst, R. R. *J. Chem. Phys.* **1979**, *71*, 4546.
(3) Kumar, Anil; Ernst, R. R.; Wüthrich, K. *Biochem. Biophys. Res. Commun.* **1980**, *95*, 1.
(4) Macura, S.; Ernst, R. R. *Mol. Phys.* **1980**, *41*, 95.
(5) Wüthrich, K. *NMR of Proteins and Nucleic Acids*; John Wiley & Sons: New York, 1986.
(6) Neuhaus, D.; Williamson, M. P. *The Nuclear Overhauser Effect in Structural and Conformational Analysis*; Verlag Chemie: Weinheim, 1989.
(7) Kalk, A.; Berendsen, H. J. C. *J. Magn. Reson.* **1976**, *24*, 343.
(8) Kumar, Anil; Wagner, G.; Ernst, R. R.; Wüthrich, K. *J. Am. Chem. Soc.* **1981**, *103*, 3654.
(9) Lane, A. N. *J. Magn. Reson.* **1988**, *78*, 425.
(10) Olejniczak, E. T.; Gampe, R. T.; Fesik, S. W. *J. Magn. Reson.* **1986**, *67*, 28.
(11) Massefski, W., Jr.; Redfield, A. G. *J. Magn. Reson.* **1988**, *78*, 150.
(12) Fejzo, J.; Westler, W. M.; Macura, S.; Markley, J. L. *J. Magn. Reson.* **1991**, *92*, 195.
(13) Vincent, S. J. F.; Zwahlen, C.; Bodenhausen, G. *Angew. Chem.*, in press.
(14) Borgias, B. A.; Gochin, M.; Kerwood, D. J.; James, T. L. *J. Magn. Reson.* **1986**, *67*, 28.
(15) Boelens, R.; Koning, T. M. G.; Kaptein, R. *J. Mol. Struct.* **1988**, *173*, 299.
(16) Fejzo, J.; Westler, W. M.; Macura, S.; Markley, J. L. *J. Am. Chem. Soc.* **1990**, *112*, 2574.
(17) Fejzo, J.; Westler, W. M.; Markley, J. L.; Macura, S. *J. Am. Chem. Soc.* **1992**, *114*, 1523.

0002-7863/94/1516-0362$04.50/0

in principle, all cross-relaxation pathways except those involving spins in a selected spectral region. This technique relies on the fact that cross-relaxation rates in the presence and absence of a resonant rf field have opposite signs in macromolecules. Using another strategy, Burghardt et al.[18] and Boulat et al.[19] have described a "synchronous nutation" method where two selected spins are driven simultaneously by two selective rf fields, allowing cross relaxation to occur only between spins in two different narrow spectral regions, other spin-diffusion pathways being suppressed. These methods tend to be elaborate and difficult to quantify, and they are susceptible to complications in the presence of J couplings and cross-correlated relaxation mechanisms.[18-21] The latter can be studied very effectively by selective spin-locking experiments, as shown by Bull,[22] by Burghardt et al.,[23] and by Brüschweiler and Ernst:[24] selective spin locking allows one to inhibit transformations of the type $\langle I_z^A\rangle \rightsquigarrow \langle I_z^X\rangle$ so that one can focus on conversion processes such as $\langle I_z^A\rangle \rightsquigarrow \langle 2I_z^AI_z^X\rangle$ which occur as a result of cross correlation between the fluctuations of dipolar couplings and chemical shift anisotropies[25] and on transformations such as $\langle I_z^A\rangle \rightsquigarrow \langle 4I_z^AI_z^KI_z^X\rangle$ which arise from cross correlation between the fluctuations of pairs of dipolar couplings.[26] Levitt and Di Bari,[20] using average Liouvillian theory,[21] have proposed schemes where π pulses are inserted in a relaxation interval in order to decouple various forms of longitudinal one- and two-spin order such as $\langle I_z^A\rangle$, $\langle I_z^X\rangle$, and $\langle 2I_z^AI_z^X\rangle$.

In this paper, we show that it is possible to study cross relaxation in a manner that is reminiscent of synchronous nutation but that is much simpler to implement and less prone to artifacts. The new method is applicable to all motional regimes (i.e., to both small and large molecules) and does not suffer from interference due to cross correlation. Our new experiment allows one to isolate a selected cross-relaxation process ($\langle I_z^A\rangle \rightsquigarrow \langle I_z^X\rangle$) while quenching spin diffusion via all other spins K, K', ... The method does not require any knowledge of the chemical shifts of the perturbing spins, although it will fail if these shifts are accidentally degenerate with those of A and X. Nevertheless, if the chemical shift of a clandestine spin K falls in the same spectral range as either A or X, its participation is restricted to the pathway A $\rightsquigarrow$ K $\rightsquigarrow$ X.

Method

Figure 1 shows an experiment for the selective measurement of the time dependence of transient Overhauser effects with suppression of spin diffusion. Much of the sequence is analogous to QUICK-NOESY (*q*uantitative *u*nravelling of *i*ntensities for *c*orroborating *k*nowledge in *n*uclear *O*verhauer *e*ffect *s*pectroscopy).[13] The sequence begins with the inversion of the longitudinal magnetization of a selected source spin A ($\langle I_z^A\rangle \rightarrow -\langle I_z^A\rangle$). This selective inversion can be achieved by Gaussian Q^3 cascade[27] applied at the chemical shift Ω_A of spin A. The initial inversion is omitted in complementary experiments (e.g., in even scans), so that the signals can be subtracted in the manner of difference spectroscopy. The longitudinal magnetization (more accurately, the deviation from thermal equilibrium) is allowed to migrate freely under the effect of cross relaxation during the first half of the mixing interval τ_m. In the middle of this relaxation time, a fraction of the magnetization has migrated from the spin A, not

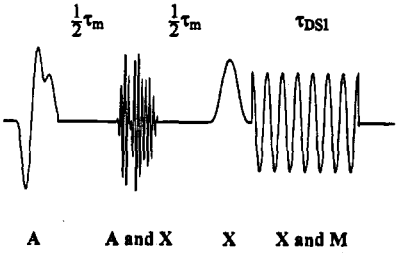

Figure 1. Sequence for the measurement of transient Overhauser effects with suppression of spin diffusion (QUIET-NOESY). The longitudinal magnetization of a selected spin A is inverted by a Q^3 Gaussian cascade applied with the radio frequency carrier set at the chemical shift Ω_A. In the middle of the relaxation or mixing interval τ_m, both the "source" spin A and the "target" spin X are inverted by an audiomodulated Q^3 Gaussian cascade, with the carrier frequency positioned at $\omega_0 = {}^1/_2(\Omega_A + \Omega_X)$ and the modulation frequency set at $\omega_a = {}^1/_2(\Omega_A - \Omega_X)$, so that the two sidebands appear at the shifts Ω_A and Ω_X. At the end of the τ_m interval, a fraction of the $\langle I_z^A\rangle$ magnetization has migrated to $\langle I_z^X\rangle$ under the effect of cross relaxation, spin diffusion via $\langle I_z^K\rangle$ being inhibited. The resulting longitudinal component $\langle I_z^X\rangle$ is converted into transverse $\langle I_x^X\rangle$ magnetization by a 270° Gaussian G^1 pulse and transferred for observation to a scalar coupled partner M ($\langle I_x^X\rangle \rightarrow \langle I_x^M\rangle$) through a homonuclear Hartmann–Hahn effect during a doubly selective irradiation period τ_{DSI}. A difference spectrum is obtained by subtracting a signal recorded without initial inversion of the A spin.

only to a target spin X ($\langle I_z^A\rangle \rightsquigarrow \langle I_z^X\rangle$) but also to various other clandestine spins K, K', ... ($\langle I_z^A\rangle \rightsquigarrow \langle I_z^K\rangle$, $\langle I_z^A\rangle \rightsquigarrow \langle I_z^{K'}\rangle$, ...), in as far as the cross-relaxation rates σ_{AK}, $\sigma_{AK'}$, ... do not vanish. The longitudinal magnetization components of both source and target spins are then inverted simultaneously ($\langle I_z^A\rangle \rightarrow -\langle I_z^A\rangle$ *and* $\langle I_z^X\rangle \rightarrow -\langle I_z^X\rangle$). This can be achieved by an audiomodulated Q^3 Gaussian cascade.[28] As discussed below, the $\langle I_z^X\rangle$ component that remains at the end of the τ_m interval is almost entirely due to the direct conversion $\langle I_z^A\rangle \rightsquigarrow \langle I_z^X\rangle$ and not to spin diffusion. In principle, it should be possible to observe this $\langle I_z^X\rangle$ magnetization directly, but in practice this may be difficult, mostly because of limitations in the accuracy of difference spectroscopy. Therefore, we resort to a form of three-dimensional spectroscopy, in the sense that we use a second mixing event. At the end of the mixing period, the longitudinal component $\langle I_z^X\rangle$ is converted into $\langle I_x^X\rangle$ by a selective 270° Gaussian G^1 pulse[29] and then transferred to a scalar-coupled "spy" nucleus M ($\langle I_x^X\rangle \rightarrow \langle I_x^M\rangle$) through a homonuclear Hartmann–Hahn effect[30,31] during a *d*oubly *s*elective *i*rradiation period τ_{DSI}. In practice, τ_{DSI} may be optimized empirically: one expects an optimum transfer for $\tau_{DSI} \approx 1/J_{MX}$ if relaxation can be neglected; otherwise the double irradiation should be made somewhat shorter. If the transfer efficiency achieved is less than 100%, this affects only the sensitivity of the experiments but not the accuracy of the buildup and decay curves.

Unlike the usual NOESY technique, where zero-quantum coherences can lead to so-called J cross peaks,[32] the method of Figure 1 does not suffer from zero-quantum artifacts, nor can it be affected by longitudinal two-spin order.[33] It is therefore possible to record spectra with a (nominally) vanishing mixing time ($\tau_m = 0$). However, we should be aware of the fact that the transfer of longitudinal magnetization may already begin *during*

(18) Burghardt, I.; Konrat, R.; Boulat, B.; Vincent, S. J. F.; Bodenhausen, G. *J. Chem. Phys.* **1993**, *98*, 1721.
(19) Boulat, B.; Burghardt, I.; Bodenhausen, G. *J. Am. Chem. Soc.* **1992**, *114*, 10679.
(20) Levitt, M. H.; Di Bari, L. *Phys. Rev. Lett.* **1992**, *69*, 3124.
(21) Levitt, M. H.; Di Bari, L. *Bull. Magn. Reson.*, in press.
(22) Bull, T. E. *J Magn. Reson.* **1991**, *93*, 596.
(23) Burghardt, I.; Konrat, R.; Bodenhausen, G. *Mol. Phys.* **1992**, *75*, 467.
(24) Brüschweiler, R.; Ernst, R. R. *J. Chem. Phys.* **1992**, *96*, 1758.
(25) Goldman, M. *J. Magn. Reson.* **1984**, *60*, 437.
(26) Fagerness, P. E.; Grant, D. M.; Kuhlmann, K. F.; Mayne, C. L.; Parry, R. B. *J. Chem. Phys.* **1975**, *63*, 2524.
(27) Emsley, L.; Bodenhausen, G. *J. Magn. Reson.* **1992**, *97*, 135.
(28) Emsley, L.; Burghardt, I.; Bodenhausen, G. *J. Magn. Reson.* **1990**, *90*, 214. Corrigendum: *Ibid.* **1991**, *94*, 448.
(29) Emsley, L.; Bodenhausen, G. *J. Magn. Reson.* **1989**, *82*, 211.
(30) Konrat, R.; Burghardt, I.; Bodenhausen, G. *J. Am. Chem. Soc.* **1991**, *113*, 9135.
(31) Zwahlen, C.; Vincent, S. J. F.; Bodenhausen, G. In *Proceedings of the International School of Physics Enrico Fermi*; B. Maraviglia, Ed.; Rome, 1993, in press.
(32) Macura, S.; Huang, Y.; Suter, D.; Ernst, R. R. *J. Magn. Reson.* **1981**, *43*, 259.
(33) Bodenhausen, G.; Wagner, G.; Rance, M.; Sørensen, O. W.; Wüthrich, K.; Ernst, R. R. *J. Magn. Reson.* **1984**, *59*, 542.

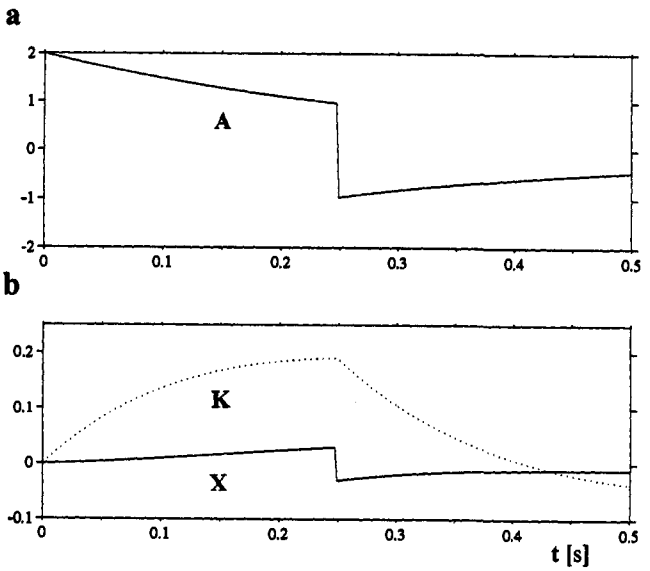

Figure 2. Simulations of the time dependence of the $\langle I_z^A \rangle$, $\langle I_z^K \rangle$, and $\langle I_z^X \rangle$ polarizations *in the course* of the relaxation interval τ_m, i.e., $0 < t < \tau_m$, when the sign of $\langle I_z^A \rangle$ and $\langle I_z^X \rangle$ is changed in the middle. The parameters of the relaxation matrix are given in the text. Note the buildup of both $\langle I_z^K \rangle$ and $\langle I_z^X \rangle$ in the first half of τ_m, which is followed by a decay in the second half of τ_m. All simulations were carried out with Matlab version 4.0 on a SUN SPARC IPX computer.

the initial inversion pulse, and further cross-relaxation processes may occur during the audiomodulated inversion pulse in the middle of the τ_m interval. These aspects will be addressed in more detail below. Because the clandestine nuclei are reduced to silence, we like to refer to the experiment of Figure 1 as QUIET-NOESY, an acronym for *q*uenching *u*ndesirable *i*ndirect *e*xternal *t*rouble in *n*uclear *O*verhauser *e*ffect *s*pectroscop*y*.

Dynamics of Spin Polarization

The mechanism of the experiment of Figure 1 may be explained either by average Liouvillian theory[20,21] or, as shown here, by simulating the time dependence of the relevant expectation values of a system with three spins A, K, and X. The relaxation dynamics are governed by the following master equation:

$$\frac{d}{dt}\begin{bmatrix}\langle I_z^A\rangle\\ \langle I_z^K\rangle\\ \langle I_z^X\rangle\end{bmatrix} = -\begin{bmatrix}\rho_A & \sigma_{AK} & \sigma_{AX}\\ \sigma_{AK} & \rho_K & \sigma_{KX}\\ \sigma_{AX} & \sigma_{KX} & \rho_X\end{bmatrix}\begin{bmatrix}\langle I_z^A\rangle - \langle I_z^A\rangle^{eq}\\ \langle I_z^K\rangle - \langle I_z^K\rangle^{eq}\\ \langle I_z^X\rangle - \langle I_z^X\rangle^{eq}\end{bmatrix}$$

In practice, since the signals are obtained from the difference between two experiments, one with and one without initial π pulse, the thermal equilibrium terms in this equation may be dropped. The expectation values which were plotted in our simulations are to be understood in the sense of difference spectroscopy as in the experiments. Figure 2 shows the time dependence of $\langle I_z^A \rangle$, $\langle I_z^K \rangle$, and $\langle I_z^X \rangle$ within a mixing interval of fixed duration $\tau_m = 0.5$ s. We have chosen $\rho_A = \rho_X = 3.02\ s^{-1}$, $\rho_K = 5\ s^{-1}$, $\sigma_{AK} = \sigma_{KX} = -1\ s^{-1}$, and $\sigma_{AX} = -0.02\ s^{-1}$. This is consistent with a system where $r_{AK} = r_{KX} < r_{AX}$ with pure dipolar relaxation in the slow tumbling limit (where $\rho_i = -\sum_j \sigma_{ij}$), with additional contributions to the diagonal elements from chemical shift anisotropy and external random fields. In the first half of the τ_m period, one observes a typical (triexponential) decay of $\langle I_z^A \rangle$, which corresponds to the τ_m dependence of the diagonal peak amplitude in NOESY. Besides the rapid buildup of $\langle I_z^K \rangle$ in Figure 2b, one observes a much slower buildup of $\langle I_z^X \rangle$, which is mostly due to a two-step process in this example, since $\sigma_{AX}\tau_m$ is much smaller than $^1/_2\sigma_{AK}\sigma_{KX}\tau_m^2$. In the middle of the mixing period in Figure 2, the signs of $\langle I_z^A \rangle$ and $\langle I_z^X \rangle$ are reversed, while $\langle I_z^K \rangle$ is not manipulated. For clarity, this sign

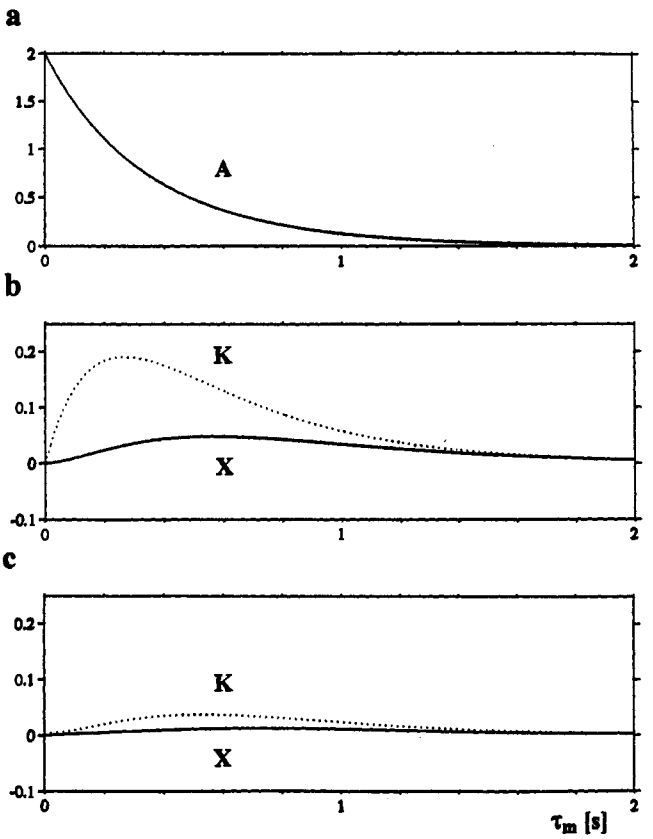

Figure 3. Comparison of the decay of $\langle I_z^A \rangle$ and the buildup of the $\langle I_z^K \rangle$ and $\langle I_z^X \rangle$ polarizations *as a function of the relaxation interval* τ_m, assuming the same rates as in Figure 2. (a) and (b) Without inversion of the magnetization during τ_m as in conventional NOESY. (c) With doubly selective inversion of A and X in the middle of τ_m.

reversal is assumed to occur instantaneously, although in practice the audiomodulated Q^3 cascade must have a finite duration and may lead to losses in signal amplitude (see below). In the second half of the mixing period, the $\langle I_z^K \rangle$ term decays: instead of receiving more polarization from the $\langle I_z^A \rangle$ bath, $\langle I_z^K \rangle$ now loses part of its order because the flow occurs in the reverse direction. The magnitude of the $\langle I_z^X \rangle$ term (deviation from zero) also decays, again because the flow of polarization, which went from K to X in the first half of τ_m, is reversed in the second half. At the end of τ_m, the polarization $\langle I_z^X \rangle$ that remains is mostly due to the direct transfer A ⇝ X and not to the two-step process A ⇝ K ⇝ X.

Figure 3 shows a comparison of buildup curves that can be obtained either without any manipulation in the course of τ_m (Figures 3a and 3b) or with doubly selective inversion of A and X (Figure 3c). Figure 3 shows the situation *at the end* of the mixing period, rather than the time dependence *during* τ_m as illustrated in Figure 2. It is clear that the transformation of $\langle I_z^A \rangle$ into both $\langle I_z^K \rangle$ and $\langle I_z^X \rangle$ is largely inhibited in Figure 3c, thus demonstrating that spin diffusion is quenched very effectively with the QUIET-NOESY sequence of Figure 1.

Experimental Examples

Oligonucleotides are known to present a challenge to structural studies using Overhauser effects, partly because the demands on accuracy tend to be greater in these systems than in proteins and partly because spin-diffusion effects are particularly severe.[11] We have studied the self-complementary palindromic DNA dodecamer $d(CGCGAATTCGCG)_2$, known as "Dickerson's dodecamer", which has been extensively studied by X-ray diffraction,[34,35] by NMR,[36] and by molecular dynamics.[37-39] Figure 4 shows two residues with arrows emphasizing cross-relaxation

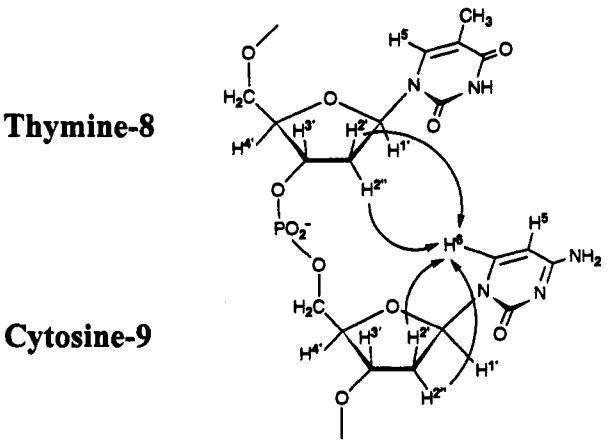

Figure 4. Thymine-8 and cytosine-9 residues in duplex d(CGCGAATTCGCG)$_2$ with indication of some cross-relaxation processes discussed in this work.

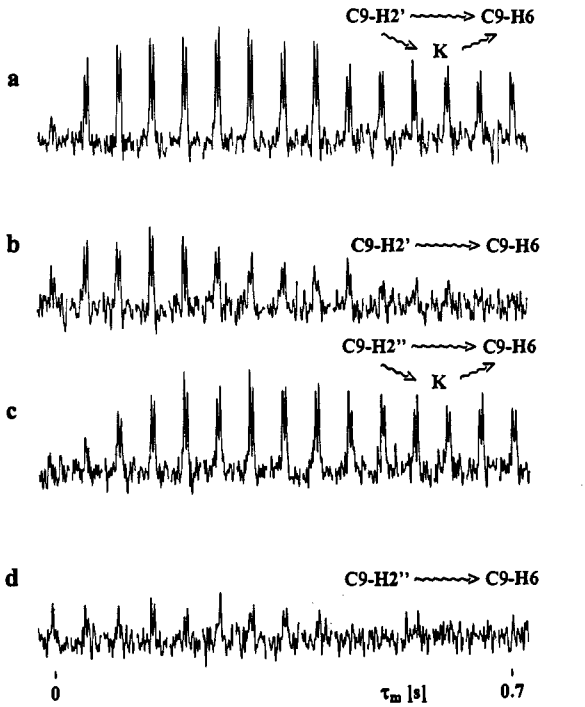

Figure 5. Selective measurements of transient Overhauser effects at 303 K in d(CGCGAATTCGCG)$_2$ duplex obtained from 3 mM d(CGCGAATTCGCG) monomer dissolved in D_2O with 100 mM sodium chloride and 10 mM phosphate buffer, pH 7.0. (a) and (b) The deoxyribose proton C9–H2′ of cytosine-9 was selectively inverted, and cross relaxation to the C9–H6 aromatic proton of the same cytosine-9 was monitored. (c) and (d) Similar to a and b, but starting with the C9–H2″ proton. In all cases, the magnetization was transferred for observation from C9–H6 to C9–H5 through a homonuclear Hartmann–Hahn effect during a doubly selective irradiation period τ_{DSI} = 131.7 ms. (a) and (c) Buildup curves obtained *without* quenching spin diffusion, recorded with the QUICK-NOESY method (i.e., by dropping the modulated Q^3 cascade from the sequence of Figure 1). (b) and (d) Buildup curves obtained *with* quenching of spin diffusion, i.e., with the QUIET-NOESY method of Figure 1. For each of the 15 values of τ_m, incremented in 50-ms steps from 0 to 700 ms, 512 scans were recorded at 1.5-s intervals, each τ_m value thus requiring 13 min. The experiments were performed with a Bruker MSL 300 spectrometer equipped with an Oxford Research Systems selective excitation unit.

pathways that have been investigated in this work. Figure 5 shows how buildup plots are affected by switching spin diffusion on or off. Figures 5a and 5c were recorded with the QUICK-NOESY scheme,[13] i.e., *without* quenching spin diffusion, and show cross-relaxation processes from two deoxyribose protons H2′ and H2″ of the cytosine-9 residue to the aromatic H6 proton of the same residue. Figures 5b and 5d show the results obtained using the QUIET-NOESY sequence of Figure 1 to quench spin diffusion. Note that the C9–H2′ ~~> C9–H6 transfer (Figure 5b) is not dramatically affected by the quenching process, whereas the C9–H2″ ~~> C9–H6 transfer (Figure 5d) is almost entirely eliminated. This proves at a glance that the former process corresponds to a "true" Overhauser effect, while the latter merely results from spin diffusion. In the latter case, we suspect that the C9–H2′ proton acts as a clandestine K proton that relays the information, i.e., that the overall pathway is H2″ ~~> H2′ ~~> H6. Such a suspicion could be corroborated by inverting H2′ rather than H2″ and H6.

In principle, if spin diffusion is quenched, our buildup plots should give a straightforward measure of the relevant cross-relaxation rates. We have therefore compared our experimental results with simulations derived from the self- and cross-relaxation rates predicted by Bolton and co-workers, given in Table 1.[40] The agreement was improved by substituting the self-relaxation rate ρ(C9–H6) = 3.48 s^{-1} predicted by molecular dynamics by a rate ρ = 4.5 s^{-1} determined by experiment. It is not surprising that self-relaxation rates derived from molecular dynamics are underestimated, since external random fields and chemical shift anisotropy are not included in the calculations. Our experiments were carried out at 300 MHz, while the predictions of Table 1 were made for 500 MHz, but this makes no significant difference. The small discrepancies between simulation and experiment apparent in Figure 6 (notably a slight time lag) can be attributed to our neglect of cross-relaxation processes that occur *during* the selective pulses.

Figure 7 shows experimental buildup plots associated with *interresidue* cross-relaxation processes from two deoxyribose protons of thymine-8 to an aromatic proton of the neighboring cytosine-9 residue. The T8–H2′ ~~> C9–H6 process seems to be largely conserved when spin diffusion is quenched, while the T8–H2″ ~~> C9–H6 conversion is completely inhibited, thus providing strong evidence that T8–H2″ is more remote than T8–H2′ from the C9–H6 proton.[41] This stands in contrast to the predictions of Bolton and co-workers,[40] who estimated that the cross-relaxation rates should be σ(T8–H2′, C9–H6) = 0.059 s^{-1} and σ(T8–H2″, C9–H6) = 0.387 s^{-1}, assuming Watson–Crick

Table 1. Relaxation Matrix[40] for Cytosine-9 in Duplex d(CGCGAATTCGCG)$_2$ Used for the Simulations of Figure 6, with Longitudinal Relaxation Rates ρ_i and Cross-Relaxation Rates σ_{ij} Expressed in s^{-1}, as Determined by Molecular Dynamics, Taking Account of Effects of Orientation, Internal Motion, and Anisotropy of the Duplex DNA[39]

	H1′	H2′	H2″	H3′	H5	H6
H1′	2.59	–0.27	–1.51	–0.06	–0.01	–0.06
H2′	–0.27	9.38	–5.50	–0.93	–0.02	–1.67
H2″	–1.51	–5.50	9.23	–0.44	0	–0.08
H3′	–0.06	–0.93	–0.44	3.60	0	–0.03
H5	–0.01	–0.02	0	0	1.38	–0.74
H6	–0.06	–1.67	–0.08	–0.03	–0.74	3.48[a]

[a] In the simulations of Figure 6, the rate ρ(C9–H6) = 4.5 s^{-1} determined by the experiment of Figure 10a was used instead.

(34) Drew, H. R.; Wing, R. M.; Takano, T.; Broka, C.; Tanaka, S.; Itakura, K.; Dickerson, R. E. *Proc. Natl. Acad. Sci. U.S.A.* **1981**, *78*, 2179.
(35) Pjura, P. E.; Grzeskowiak, K.; Dickerson, R. E. *J. Mol. Biol.* **1987**, *197*, 257.
(36) Hare, D. R.; Wemmer, D. E.; Chou, S.-H.; Drobny, G. P.; Reid, B. R. *J. Mol. Biol.* **1983**, *171*, 319.
(37) Nerdal, W.; Hare, D. R.; Reid, B. R. *Biochemistry* **1989**, *28*, 10008.
(38) Swaminathan, S.; Ravishankar, G.; Beveridge, D. L. *J. Am. Chem. Soc.* **1991**, *113*, 5027.
(39) Withka, J. M.; Swaminathan, S.; Beveridge, D. L.; Bolton, P. H. *J. Am. Chem. Soc.* **1991**, *113*, 5041.
(40) Bolton, P. H., private communication.
(41) The assignment of the T8–H2′ and T8–H2″ protons is established beyond doubt, since J(H2′H1′) ≫ J(H2″H1′), as confirmed by Hartmann–Hahn experiments.

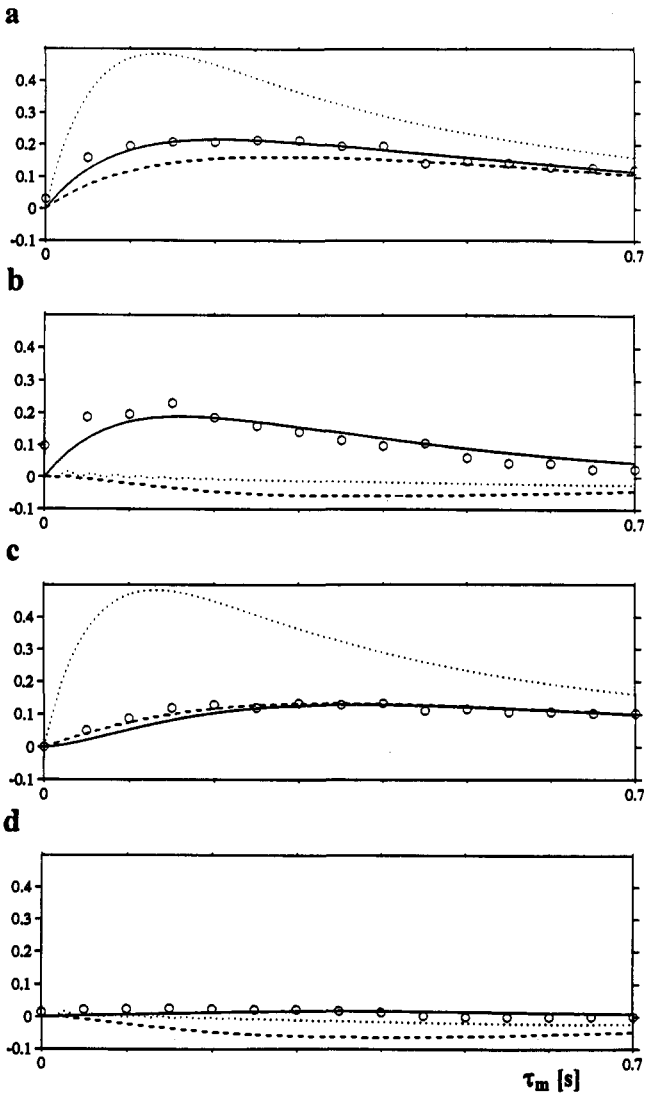

Figure 6. Simulations corresponding to the experimental observations of Figure 5, assuming that the population dynamics are adequately described by considering only six spins and based on the self- and cross-relaxation rates of Table 1, except for one self-relaxation rate which was determined experimentally. (a) Transfer C9–H2′ ⇝ C9–H6 with spin diffusion as can be monitored by NOESY or QUICK-NOESY. (b) Transfer C9–H2′ ⇝ C9–H6 without spin diffusion as can be observed by QUIET-NOESY. (c) Transfer C9–H2″ ⇝ C9–H6 with spin diffusion. (d) Transfer C9–H2″ ⇝ C9–H6 without spin diffusion. Circles represent experimental amplitudes, the vertical scale being adjusted so that the measurements coincide with the simulated curves at 0.25 s in a, 0.2 s in b, and 0.35 s in c and d. Solid curves represent the target spin C9–H6, dashed curves C9–H3′. Dotted curves represent C9–H2″ in a and b, C9–H2′ in c and d. Relaxation processes during the initial inversion and subsequent doubly selective inversion pulses were not taken into account.

pairing with effects of orientation, anisotropy of the overall motion, and the presence of local mobility.[39]

Relaxation during Selective Pulses

The simulations of Figure 6 show idealized situations, where the magnetization vectors of the A and X spins are assumed to be inverted instantaneously without any losses. In actual fact, the audiomodulated Q^3 pulses used for this purpose, which must perfectly invert magnetization within spectral widths of about 70 Hz, typically have a duration on the order of 35 ms.[27] The bandwidth must be wide enough to cover the full width of the multiplets but narrow enough to be unlikely to affect any other spins K, K′, ... Because of the finite duration of the pulses, there are unavoidable losses of magnetization through longitudinal and

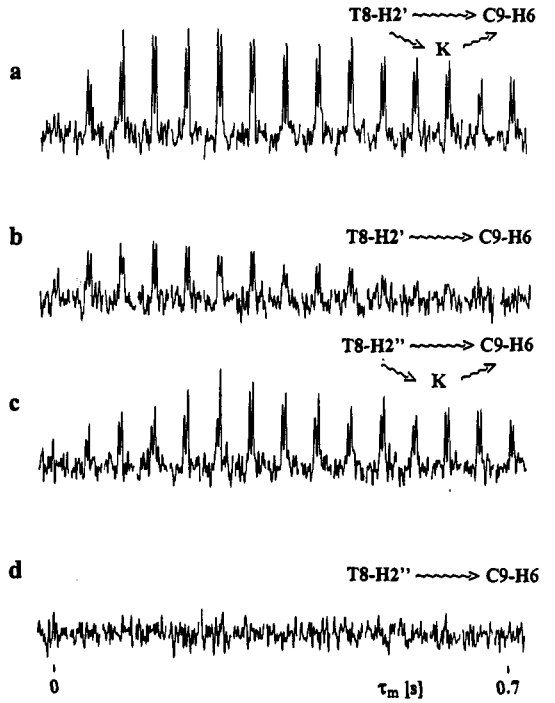

Figure 7. Selective measurements of transient Overhauser effects in duplex d(CGCGAATTCGCG)$_2$ similar to Figure 5. (a) The deoxyribose H2′ proton of thymine-8 was selectively inverted, and cross relaxation to the aromatic H6 proton of the neighboring cytosine-9 was monitored by QUICK-NOESY without quenching spin diffusion. (b) Same process, but with suppression of spin diffusion with QUIET-NOESY. (c) Cross relaxation from T8–H2″ to C9–H6 without quenching. (d) Same process, but with suppression of spin diffusion. In all cases, the magnetization was transferred to C9–H5 through a homonuclear Hartmann–Hahn effect as in Figure 5.

transverse relaxation.[42,43] We have developed complementary experiments designed to measure these losses, so that they can be compensated for by calibration. The simplest solution consists of applying *two consecutive* audiomodulated Q^3 pulses in the middle of the mixing interval. Because two inversions amount to a unity operation, this sequence is inoperative in the sense that it fails to quench spin diffusion. If there were no losses during the pulses, the buildup curves should therefore be the same as in the basic QUICK-NOESY sequence, i.e., when the doubly selective inversion pulses are skipped altogether. However, if each audiomodulated Q^3 pulse entails a loss of longitudinal magnetization given by a factor k (typically $0.7 < k < 0.9$, depending on the T_1 and T_2 relaxation times and on the rf inhomogeneity), two consecutive inversions will lead to an attenuation factor k^2, provided appropriate phase cycling is used to remove undesirable transverse magnetization components. Figure 8 shows a comparison of buildup plots obtained in this manner, which leads us to estimate that $k \approx 0.8$ in this example. In addition to the overall attenuation, one observes an enhancement of the signals in Figure 8b for the (nominal) value $\tau_m = 0$. This must be due to cross relaxation ($\langle I_z^A \rangle$ ⇝ $\langle I_z^X \rangle$) that occurs *during* the two consecutive double inversion pulses, which leads to a time shift of the origin of the τ_m domain.

Perhaps a more straightforward comparison is possible between two different experiments that *both* incorporate two inversion pulses, so that the losses are the same. One sequence uses two consecutive amplitude-modulated Q^3 inversion pulses, so that spin diffusion is not quenched; the other uses two similar pulses, but situated at one-quarter and three-quarters of τ_m. It may

(42) Hajduk, P. J.; Horita, D. A.; Lerner, L. *J. Magn. Reson. Ser. A* **1993**, *103*, 40.
(43) Horita, D. A.; Hajduk, P. J.; Lerner, L. *J. Magn. Reson. Ser. A* **1993**, *103*, 53.

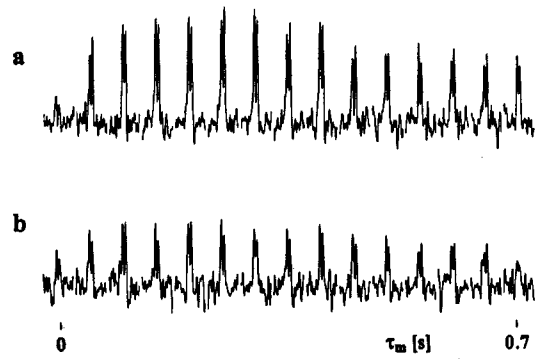

Figure 8. (a) Transfer C9–H2′ ⇝ C9–H6 in duplex d(CGCGAATTCGCG)$_2$ recorded by QUICK-NOESY without quenching spin diffusion. (b) Same process, again recorded without quenching spin diffusion, but with two consecutive doubly selective inversion pulses in the middle of the relaxation period (see text). Apart from an attenuation factor k^2 and a slight shift along the time axis, the envelope is comparable to a. The comparison allows one to estimate that $k = 0.8$ for each amplitude-modulated Q^3 cascade.

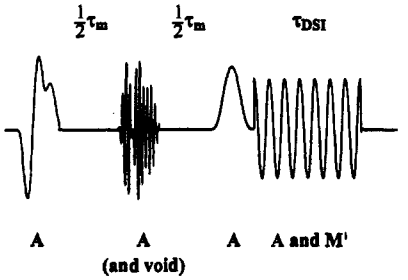

Figure 9. Sequence for the measurement of the decay of longitudinal magnetization with suppression of spin diffusion. The $\langle I_z^A \rangle$ magnetization is first inverted by a Q^3 Gaussian cascade. In the middle of τ_m, one of the sidebands of the audiomodulated Q^3 Gaussian cascade inverts $\langle I_z^A \rangle$ again, while the other sideband is positioned outside the spectrum (in the "void"). At the end of the τ_m interval, the remaining $\langle I_z^A \rangle$ magnetization is first converted into transverse $\langle I_x^A \rangle$ magnetization by a 270° Gaussian G^1 pulse and then transferred to a scalar coupled partner M′ ($\langle I_x^A \rangle \rightarrow \langle I_x^{M'} \rangle$) through a homonuclear Hartmann–Hahn effect. A difference spectrum is obtained by subtracting a signal recorded without initial inversion of the A spin.

be shown by average Liouvillian theory[20,21] that these timings lead to optimal suppression of undesirable pathways. If we compare these two experiments directly, there is no need for any calibration, but the sensitivity of the signals is reduced by a factor k^2 in both cases. The second sequence is analogous to an experiment proposed by Levitt and Di Bari.[20] As these authors have pointed out, the degree of quenching is improved by repeated inversion. However, in homonuclear systems, it must be borne in mind that the duration of a selective π pulse is not negligible on the time scale of cross relaxation and that it is not so simple to ascertain the amount of magnetization that is transferred during the pulses. In addition, if we use n modulated pulses, the signal will be attenuated by a factor k^n. For these reasons, we tend to prefer a comparison between buildup plots such as those shown in Figure 8 to estimate the factor k, so that we can use this factor in comparing plots such as those in Figures 5a and 5b.

Degeneracies

So far, we have tacitly assumed that it is possible to invert the longitudinal magnetization components of two selected spins A and X without affecting any other spins in the molecule. In crowded spectra, this is a mere abstraction, since the doubly selective pulses invert many magnetization components with chemical shifts in the vicinity of A and X. Fortunately, this is completely irrelevant to the outcome of the experiment, except if by a stroke of bad luck a spin K which is dipole-coupled to both

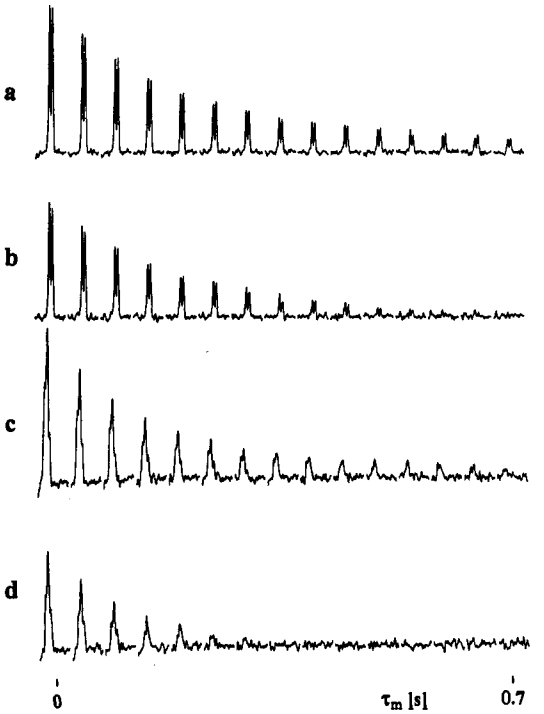

Figure 10. (a) Decay of the polarization of the aromatic C9–H6 proton of cytosine-9 in duplex d(CGCGAATTCGCG)$_2$, measured *without* inversion using QUICK-NOESY adapted for diagonal peak measurement, i.e., with both the initial inversion pulse and the 270° pulse applied to the same nucleus. (b) Same C9–H6 proton, measured *with* inversion using QUIET-NOESY adapted for diagonal peak measurements (Figure 9). (c) Decay of the deoxyribose C9–H2′ proton of the same cytosine-9, measured *without* inversion. (d) Same C9–H2′ proton, measured *with* inversion. Although only one proton needs to be inverted in experiments b and d, and audiomodulated Q^3 pulse was employed, with the low-frequency sideband applied at the chemical shifts of the C9–H6 and C9–H2′ protons, respectively, and the high-frequency sideband well outside the spectrum. Note the apparent enhancement of the relaxation rates in b and d. In a and b, the magnetization was transferred for observation by a homonuclear Hartmann–Hahn effect to the C9–H5 proton (τ_{DSI} = 131.7 ms); in c and d to the C9–H1′ proton (τ_{DSI} = 64.8 ms).

A and X happens to be inverted unwittingly. In other words, if a spin K which has a position in the molecule that makes it capable of transmitting magnetization $\langle I_z^A \rangle$ ⇝ $\langle I_z^K \rangle$ ⇝ $\langle I_z^X \rangle$ happens to be nearly degenerate in terms of chemical shifts with either A or X, spin diffusion mediated through K is *not* inhibited. This situation could easily occur for diastereotopic protons in CH_2 groups whenever the environment is such that the two protons are nearly degenerate.

Decay of Diagonal Peaks

We have demonstrated elsewhere[13] that QUICK-NOESY can be used to monitor the decay of the longitudinal magnetization of a selected proton in a manner that is equivalent to measuring the time dependence of a diagonal peak in NOESY. Such measurements and their interpretation have been discussed by Boulat et al.[44] In this section, we discuss a variant of this experiment, which is obtained by inverting the A spin in the middle of the τ_m interval, as shown in Figure 9. We use a modulated Q^3 pulse in such a manner that one sideband acts on the A spin while the other sideband is applied well outside the spectrum, or in the "void".[18] This makes comparisons straightforward without the need of recalibrating pulse amplitudes. As shown in Figures 10b and 10d, this procedure leads to a significant *acceleration* of the decay of the longitudinal magnetization, compared to the experiments of Figures 10a and 10c, where the A magnetization is not inverted in the τ_m interval. Since we are

(44) Boulat, B.; Bodenhausen, G. *J. Biomol. NMR* **1993**, *3*, 335.

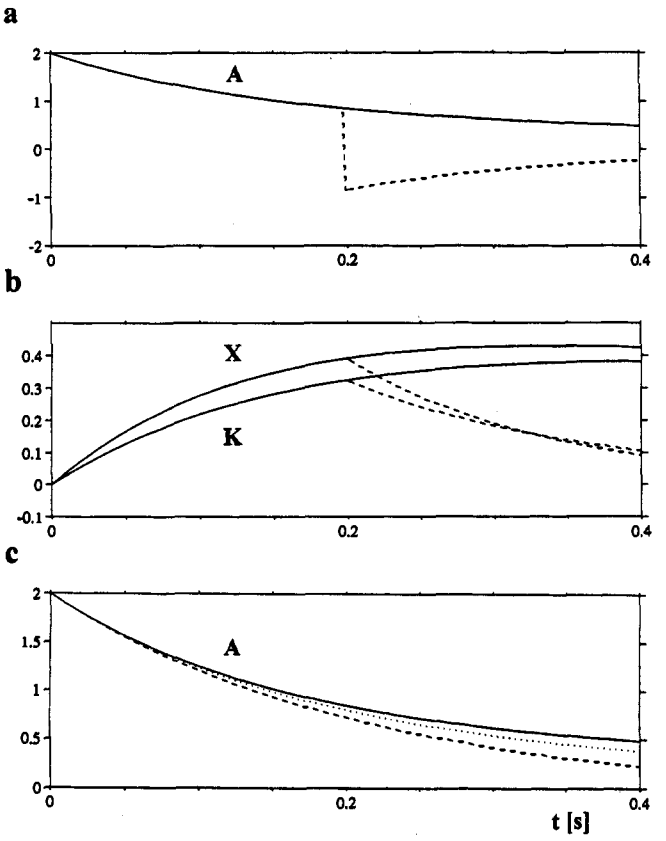

Figure 11. Simulations of the time evolution of the polarization, i.e., $0 < t < \tau_m$, with different manipulations in the middle of the relaxation interval τ_m. The elements of the relaxation matrix are given in the text. (a) Time dependence of $\langle I_z^A \rangle$ in the course of τ_m without inversion (solid line) and with inversion of A only (dashed line). (b) Evolution of $\langle I_z^K \rangle$ and $\langle I_z^X \rangle$ without inversion (solid lines) and with inversion of A only (dashed lines). (c) Amplitude of $\langle I_z^A \rangle$ at the end of τ_m for three cases: (i) no inversion (solid line), (ii) inversion of both A and X (dotted line), and (iii) inversion of A alone (dashed line).

concerned with difference experiments, where the magnetization behaves as if it were relaxing to a completely demagnetized state (rather than to thermal equilibrium), the sign reversal should not affect the decay rate if the lattice had an infinite heat capacity. In the context of dipolar relaxation, however, we must consider the heat capacity of the neighboring spins, which constitutes a bottleneck. This point is best understood by considering the simulations of Figure 11, which refer to a 3-spin system, calculated with $\rho_A = 5\ s^{-1}$, $\rho_K = 3\ s^{-1}$, $\rho_X = 3.5\ s^{-1}$, $\sigma_{AK} = -1.5\ s^{-1}$, $\sigma_{KX} = -1\ s^{-1}$, and $\sigma_{AX} = -2\ s^{-1}$. Spins K and X act as two "heat sinks" to spin A. Apart from the decay of $\langle I_z^A \rangle$ in Figure 11a, one observes how order is building up in the $\langle I_z^K \rangle$ and $\langle I_z^X \rangle$ reservoirs (Figure 11b). After inversion of A only, the $\langle I_z^K \rangle$ and $\langle I_z^X \rangle$ terms decay again, because the direction of the flow is reversed. As a result, the (negative) polarization of the A spin returns more rapidly to the demagnetized state than in the control experiments, where the A spin is not manipulated. This can be appreciated in Figure 11c, which illustrates the τ_m dependence of $\langle I_z^A \rangle$ under three different scenarios: (i) no inversion at all (or, equivalently, inversion of all three spins), (ii) inversion of A and X (or, equivalently, inversion of K only), and (iii) inversion of A only (or, equivalently, inversion of both K and X). It is clear that, if only A is inverted selectively, its decay is accelerated in proportion to the number of spins that are available to act as heat sinks. This type of experiment may help to obtain a more detailed picture of relaxation pathways.

Conclusions

We have presented an efficient method that allows one to measure cross-relaxation rates between two selected spins A and X without significant interference due to spin-diffusion processes. The technique should open the way to more accurate measurements of cross-relaxation rates σ_{AX} and hence to more reliable estimates of internuclear distances r_{AX}, including perhaps longer distances of up to, say 3 or 4 Å. The methods are intended to refine distances derived from nonselective NOESY experiments, and they are suitable not only for proteins, protein/DNA complexes, and other macromolecular assemblies but also for small molecules, either in isolation or bound to a larger receptor.

Acknowledgment. We gratefully acknowledge Dr. Philip Bolton (Wesleyan, CT) and Dr. Jane Withka (Pfizer, New London, CT) for a sample of d(CGCGAATTCGCG)$_2$, many helpful discussions, and providing the information on relaxation rates in Table 1. M.H.L. is grateful for stimulating discussions with Dr. Mary Roberts and Dr. Anil Kumar, and G.B. acknowledges suggestions by Dr. Carol Post and careful reading of the manuscript by Dr. Benoit Boulat. This research was supported by the Fonds National de la Recherche Scientifique (FNRS), by the Commission pour l'Encouragement de la Recherche Scientifique (CERS) of Switzerland, and by the Swedish Natural Science Research Council (L.D.B. and M.H.L.).